50th AIAA Aerospace Sciences Meeting including the New Horizons Forum and Aerospace Exposition
09 - 12 January 2012, Nashville, Tennessee

AIAA 2012-0967

# Efficient Kriging-Based Aerodynamic Design of Transonic Airfoils: Some Key Issues

Jun Liu [*], Zhong-Hua Han [†] and Wen-Ping Song [‡].
*National Key Laboratory of Science and Technology on Aerodynamic Design and Research, School of Aeronautics, Northwestern Polytechnical University, Xi'an, 710072, P .R. China*

Downloaded by TURKISH AEROSPACE INDUSTRIES (TAI) on May 2, 2023 | http://arc.aiaa.org | DOI: 10.2514/6.2012-967

**Today's complex time-consuming Computational Fluid Dynamics (CFD) codes stimulated the use of surrogate models in aerodynamic design. In this paper, an efficient Kriging-based airfoil design system is developed, including functionalities of optimization design and inverse design. In this system, Design of Experiment techniques are used to select initial sample points in the design space and initial Kriging models are subsequently built for the cost function as well as the constraints, based on the sampled data; the Kriging models are refined repetitively by minimizing the Kriging approximated cost function or maximizing its Expected Improvement (EI) with genetic algorithm, until the global optimum is found. Four key issues about the design system is investigated: First, the performance of global optimization is tested for an analytical problem with extremely poor initial sampling; Second, the number of function evaluation needs to explore the global optimum for an analytical function is investigated with the number of design variables ranging from 2 to 40; Third, the optimization system is compared with the conventional quadratic response surface method (RSM) in drag minimization of transonic airfoil, which confirms that the Kriging-based optimization outperforms RSM method both in efficiency and percentage of drag reduction; Fourth, the design system is demonstrated for inverse design of a transonic airfoil, which also shows that it is very efficient and robust.**

## Nomenclature

| | | |
|---|---|---|
| *Area* | = | area of the airfoil |
| *Thickness* | = | maximum thickness of the airfoil |
| $c_l$ | = | lift coefficient |
| $c_d$ | = | drag coefficient |
| $c_m$ | = | moment coefficient |
| $C_p$ | = | pressure coefficient |
| $C_{p0}$ | = | pressure coefficient of the target airfoil |
| $c$ | = | chord length of the airfoil |
| Ma | = | Mach number of the flow |
| Re | = | Reynolds number of the flow |
| $\alpha$ | = | angle of attack |
| **W** | = | conservative variables in the Reynolds-Averaged Navier-Stocks equations |
| **E**, **F** | = | invicid flux term in the Reynolds-Averaged Navier-Stocks equations |
| $\mathbf{E}_v$, $\mathbf{F}_v$ | = | viscous flux term in the Reynolds-Averaged Navier-Stocks equations |
| $n_s$ | = | number of samples |
| $n_v$ | = | number of design variables |
| $n_s^{ini}$ | = | initial number of samples |
| $n^{add}$ | = | number of samples added to the initial samples |

[*] Ph.D Student, P.O. Box 754, School of Aeronautics, Youyi West Road, No.127, Xi'an; 470381562@qq.com.
[†] Associate Professor, P.O. Box 754, School of Aeronautics, Youyi West Road, No.127, Xi'an; hanzh@nwpu.edu.cn, AIAA member.
[‡] Professor, P.O. Box 754, School of Aeronautics, Youyi West Road, No.127, Xi'an; wpsong@nwpu.edu.cn.



Copyright © 2012 by the American Institute of Aeronautics and Astronautics, Inc. All rights reserved.

$Y, G$ = random function
$\beta$ = zero-order regression model for Kriging model
$Z(\bullet)$ = Gaussian random processes
$\sigma^2$ = process variance
R = correlation function
$\mathbf{x}$ = site in the design space
$\mathbf{R}$ = correlation matrix
$\boldsymbol{r}$ = correlation vector
$\boldsymbol{\theta}$ = spatial correlation function coefficients
$\boldsymbol{w}$ = Kriging weight
$\boldsymbol{y}_s$ = observed data of the samples
$\mathbf{1}$ = unit column vector
$s^2$ = mean squared error

*Superscripts*

^ = predicted value of the parameter
$(i),(j)$ = $\in [1, n_s]$

*Subscripts*

$k$ = $\in [1, n_v]$

Downloaded by TURKISH AEROSPACE INDUSTRIES (TAI) on May 2, 2023 | http://arc.aiaa.org | DOI: 10.2514/6.2012-967

## I. Introduction

WITH the rapid development of high-performance computing, the high-fidelity CFD codes such as Reynolds-Averaged Navier-Stocks (RANS) codes have been widely applied to aerodynamic design of aircraft. The CFD-based aerodynamic design methods can be mainly categorized into two classes: optimization design and inverse design. For an optimization design problem, the optimum shape is found by minimizing (or maximizing) the objective function related to the concerned aerodynamic performance (such as drag or lift-to-drag ratio), subject to geometric and aerodynamic constraints; whereas for an inverse design problem, the optimum shape is usually determined by minimize the difference between current and target pressure distributions. To meet the performance requirements of a realistic aerodynamic design problem, the designer usually needs to perform both optimization and inverse designs in a repetitive way. Hence, an aerodynamic design system needs to have both functionalities of optimization and inverse design. From an optimization point of view, both optimization design and inverse design need to solve an optimization problem by coupling optimization algorithms with CFD simulation codes. When high-fidelity thus time-consuming CFD codes are employed, the optimization procedure becomes demanding. Therefore, efficient and robust optimization algorithms are of great importance for an aerodynamic design system.

The optimization algorithms used in aerodynamic design can be classified into two categories: gradient-based methods and evolutionary algorithms such as genetic algorithms (GAs). A gradient-based method is usually very efficient. It crucially depends on the computation of gradient. The adjoint method allows the extremely efficient computation of gradient, in which the computation cost is essentially independent of the number of design variables. Therefore, adjoint-based method rapidly gained popularity in aerodynamic optimization. Although the adjoint-based method is very efficient, it is still a local optimization method and can't find the global optimum, especially in case of flows with high nonlinearity. It is well known that the design space of a typical aerodynamic optimization is essentially multi-modal. Global optimization methods such as Genetic Algorithm (GAs) are thus of great interest. However, direct incorporation of GAs in high-fidelity CFD-based aerodynamic design optimization suffers from the extremely large computational cost, which may make it computationally prohibitive.

In light of these, a new type of optimization method, surrogate-based optimization, was introduced for aerodynamic design optimization and was demonstrated to be very effective. The use of surrogate models is playing an increasingly important role in aerodynamic design. An overview of surrogates and recent advances in surrogate-based optimization was presented by Forrester[1]. Among all the surrogate models, Kriging is one of the most popular methods, because it can represent high nonlinear functions and give error prediction which is crucial for the model refinement and the search of the global optimum. Recently, the Kriging combined with expected improvement (EI) method is widely used in aerodynamic or multidisciplinary optimization[2-8]. Although Kriging-based optimization has received increasing attentions, it does not mature enough before a number of key issues below are sufficiently addressed:

1) First, the verification of global optimization. Although the Kriging with EI is regarded as a global optimization method[13], there is little research confirms this in the numerical optimization problems. Hence, further research should be done. And this paper gives a numerical example to further convince us its globality.

2) Second, the problem of the size. As we know that, there is a so-called "curse of dimensionality" in the surrogate-based optimization, i.e. the number of sample points (function evaluations) grows rapidly as the number of design variables is increased. It is known that the number of sample points of fitting a quadratic response surface model (RSM) grows proportional to $n_v^2$ ( $n_v$ is the number of dimensionality), which quickly becomes prohibitive for high dimensional problems. While in the case of Kriging model, there is no research revealed how the problem of the size grows with the increasing of dimensionality. Hence, this paper also aims to address this issue.

3) Third, comparison of surrogate models for optimization. There are some researches in which the surrogate models are compared in aerodynamic and multidisciplinary optimization. Simpson[15] compared the response surface and Kriging for the Aerospike nozzle optimization. They found that the RMS and Kriging is comparable, and the RSM is somewhat better than the Kriging. Peter[16] compared different surrogate models for the optimization of 2D turbomachinery flow. They found that Kriging and radial basis function (RBF) is better than others. Nevertheless, both of these researches didn't take advantage of the error estimation of the Kriging. Paiva[9] compared RSM with Kriging and Artificial Neural Networks (ANN) in a multidisciplinary wing design, and used the trust region method to refine the models. They found that the RSM is only suited for very simple problems. In this research, an efficient Kriging-based optimization framework is established and compared with the iterative RSM-based optimization method, which shows that Kriging-based method outperforms RSM-based method both for efficiency and efficacy.

4) Forth, feasibility for inverse design. Inverse aerodynamic design is usually implemented by gradient-based optimization methods. From a general point of view, as an optimization method, the surrogate-based optimization can be utilized in the inverse design. Xiong Juntao[11] employed the response surface method in the aerodynamic inverse airfoil design. This paper presents a Kriging-based inverse design method to confirm the capability of Kriging model in the inverse airfoil design, both for single- and multi-point design.

## II. Flow Analysis

The flow analyses are performed with the in-house code called PMNS2D. It solves the Reynolds-Averaged Navier-Stocks (RANS) equations to simulate the flows around the airfoils. The two dimensional RANS equations used in PMNS2D is as follows:

$$\frac{\partial \mathbf{W}}{\partial t}+\frac{\partial \mathbf{E}}{\partial x}+\frac{\partial \mathbf{F}}{\partial y}=\frac{\partial \mathbf{E}_v}{\partial x}+\frac{\partial \mathbf{F}_v}{\partial y}, \tag{1}$$

where $\mathbf{W}$ is conservative variables, $\mathbf{E}$ and $\mathbf{F}$ are the invicid flux term, $\mathbf{E}_v$ and $\mathbf{F}_v$ are the viscous flux term. The equations are solved on structured meshes, using the cell centered finite volume approach. The second-order Jameson's central scheme is used as spatial scheme. The Spalart-Allmaras one-equation turbulence model is used for turbulence flow simulation. Implicit residual smoothing, local time-stepping and multigrid techniques are used to accelerate the solution to convergent to the steady state.

## III. Kriging-Based Optimization System

### A. Kriging Model

Kriging is a statistical interpolation method suggested by Krige[17] in 1951 and mathematically formulated by Matheron[18] in 1963. Kriging was widely used in the context of geostatistical problems. In 1989, Kriging was extended by Sacks et al[19] for the design and analysis of deterministic computer experiments. Then it was widely used as a surrogate modeling technique for predicting the output of computer codes in simulation-based analysis and optimization. The ordinary Kriging is used in this paper.

1) Kriging Predictor and Mean Squared Error

The Kriging treats the output of a deterministic computer experiment as a constant term plus a stochastic process:

$$Y(\mathbf{x})=\beta+Z(\mathbf{x}). \tag{2}$$

The stationary random process $Z(\bullet)$ has mean zero and covariance of



Downloaded by TURKISH AEROSPACE INDUSTRIES (TAI) on May 2, 2023 | http://arc.aiaa.org | DOI: 10.2514/6.2012-967

$$Cov[Z(\mathbf{x}),Z(\mathbf{x}')]=\sigma^2 R(\mathbf{x},\mathbf{x}'), \tag{3}$$

where $\sigma^2$ is the process variance of $Z(\bullet)$ (it is assumed that $\sigma^2(\mathbf{x})\equiv\sigma^2$ for all $\mathbf{x}$, and $R$ is the spatial correlation function that only depends on the Euclidean distance between two sites $\mathbf{x}$ and $\mathbf{x}'$.

We assume that the output of a computer code can be approximated by a linear combination of the observed data $\mathbf{y}_S$, the Kriging approximation of $y(\mathbf{x})$ at an untried $\mathbf{x}$ is formally defined as

$$\hat{y}(\mathbf{x})=\sum_{i=1}^{n_s} w_i y_i=\mathbf{w}^{\mathrm{T}}\mathbf{y}_S, \tag{4}$$

where $\mathbf{w}=(w^{(1)},...,w^{(n_s)})^{\mathrm{T}}$ are the weight coefficients (called Kriging weights). We replace $\mathbf{y}_S=(y^{(1)},...,y^{(n_s)})^{\mathrm{T}}$ with the corresponding random quantities $\mathbf{Y}_S=(Y^{(1)},...,Y^{(n_s)})^{\mathrm{T}}$.

By minimizing the Mean Squared Error (MSE) of this predictor, we can obtain the following Kriging predictor

$$\hat{y}(\mathbf{x})=\hat{\beta}+\mathbf{r}^{\mathrm{T}}(\mathbf{x})\mathbf{R}^{-1}(\mathbf{y}_s-\mathbf{1}\hat{\beta}), \tag{5}$$

where $\mathbf{1}$ is unit column vector filled with ones and

$$\hat{\beta}=\left(\mathbf{1}^{\mathrm{T}}\mathbf{R}^{-1}\mathbf{1}\right)^{-1}\mathbf{1}\mathbf{R}^{-1}\mathbf{y}_S, \tag{6}$$

and

$$\mathbf{R}:=\left[R(\mathbf{x}^{(i)},\mathbf{x}^{(j)})\right]_{ij}\in\mathbb{R}^{n\times n},\mathbf{r}(\mathbf{x}):=\left[R(\mathbf{x}^{(i)},\mathbf{x})\right]_i\in\mathbb{R}^n. \tag{7}$$

The MSE of the Kriging prediction at any untried $\mathbf{x}$ can be proven to be

$$MSE[\hat{y}(\mathbf{x})]=\hat{\sigma}^2[1-\mathbf{r}^{\mathrm{T}}\mathbf{R}^{-1}\mathbf{r}+(1-\mathbf{1}\mathbf{R}^{-1}\mathbf{r})^2/\mathbf{1}^{\mathrm{T}}\mathbf{R}\mathbf{1}], \tag{8}$$

where

$$\hat{\sigma}^2=\frac{1}{n_s}(\mathbf{y}_s-\mathbf{1}\hat{\beta})^{\mathrm{T}}\mathbf{R}^{-1}(\mathbf{y}_s-\mathbf{1}\hat{\beta}). \tag{9}$$

2) Correlation Models

The construction of the correlation matrix $\mathbf{R}$ and the correlation vector $\boldsymbol{r}$ requires the calculation of the correlation functions. The correlation function for random variables at two sites $\mathbf{x}^{(i)},\mathbf{x}^{(j)}$ is assumed to be only dependent on the spatial distance. From an engineer's point of view, the correlation models for Kriging model should have the following features: 1)Approach 1 when the distance approaches 0; 2) Decrease smoothly with the increase of distance; 3) Approach 0 when the distance approaches infinite; 4) At least one-order differentiable. Here we focus on a family of correlation models that are of the form

$$R(\mathbf{x}^{(i)},\mathbf{x}^{(j)})=\prod_{k=1}^{n_v}R_k(\theta_k,\mathbf{x}_k^{(i)}-\mathbf{x}_k^{(j)}). \tag{10}$$

The correlation function used here is the cubic spline:

$$R_k=\begin{cases}1-15\xi_k^2+30\xi_k^3 & \text{for } 0\le\xi_k\le 0.2\\ 1.25(1-\xi_k)^3 & \text{for } 0.2<\xi_k<1\\ 0 & \text{for } \xi_k\ge 1\end{cases},\ \text{where } \xi_k=\theta_k\left|\mathbf{x}_k^{(i)}-\mathbf{x}_k^{(j)}\right|. \tag{11}$$

3) Kriging Fit

Hyper parameters of Kriging, $\boldsymbol{\theta}=(\theta_1,...,\theta_{n_v})$, can be tuned by solving Maximum Likelihood Estimation (MLE) problem:

$$\text{MLE}=\arg\max_{\boldsymbol{\theta}}\left(-\frac{1}{2}\left[n_s\ln(\hat{\sigma}^2)+\ln|\mathbf{R}|\right]\right). \tag{12}$$



Downloaded by TURKISH AEROSPACE INDUSTRIES (TAI) on May 2, 2023 | http://arc.aiaa.org | DOI: 10.2514/6.2012-967

In this paper, the quasi-Newton method is used.

### B. Infill Criteria

After the surrogate model is constructed, the global optimum may not be found, since the model is not accurate. Additional points should be infilled both to increase the accuracy of the model and to explore the design space. In this paper, multiple infill strategies[1, 14] can be switched or implemented simultaneously.

1) Constrained Expected Improvement ($EI_c$)[1]

Expected improvement is defined as the improvement we expect to achieve at an untried site $\mathbf{x}$. Assume the random variable $Y \sim N[\hat{y}(\mathbf{x}), s^2(\mathbf{x})]$, where $\hat{y}$ is the Kriging predictor defined in Eq. (5), $s^2$ is mean square error defined in Eq. (8). Let $y_{\min}$ is the current best objective function value; the improvement is $I = y_{\min} - Y(\mathbf{x}) > 0$. The expected improvement is given by

$$E[I(\mathbf{x})] = \begin{cases} (y_{\min} - \hat{y}(\mathbf{x}))\Phi\left(\frac{y_{\min} - \hat{y}(\mathbf{x})}{s(\mathbf{x})}\right) + \mathrm{s} \times \phi\left(\frac{y_{\min} - \hat{y}(\mathbf{x})}{s(\mathbf{x})}\right) & \text{if } \mathrm{s}>0 \\ 0 & \text{if } \mathrm{s}=0 \end{cases}, \tag{13}$$

where $\Phi(\bullet)$ and $\phi(\bullet)$ are the cumulative distribution function and probability density function of standard normal distribution, respectively.

Assume we have a constraint $g(\mathbf{x}) > g_{\min}$, and we also constructed a Kriging model for $g(\mathbf{x})$. Following the same logic of the expected improvement, we assume the random variable $G \sim N[\hat{g}(\mathbf{x}), s^2(\mathbf{x})]$. Then, the probability that the constraint is fulfilled is as following:

$$P[G > g_{\min}] = \Phi\left(\frac{g_{\min} - \hat{g}(\mathbf{x})}{s(\mathbf{x})}\right), \tag{14}$$

where $s$ is the variance of the Kriging Model of the constraint. Then, the constrained expected improvement is:

$$E_c[I(\mathbf{x})] = E[I(x) \cap G > g_{\min}] = E[I(\mathbf{x})] \bullet P[G > g_{\min}]. \tag{15}$$

For multiple constraints, the constrained expected improvement is obtained by multiplying each probability that the constraints fulfilled.

The greater the $EI_c$, the more improvement we expect to achieve, thus the point with maximum $EI_c$ is found then observed and infilled to the sample set to refine the Kriging model. This criteria is considered a type of "balanced exploration and exploitation"[1].

2) Minimizing the Predictor (MP)

This criterion assumes that the surrogate model is globally accurate and we only need to validate the optimum of the surrogate. The optimum point on the surrogate is found and observed to refine the Kriging model. It is considered a type of "exploitation"[1]. In this paper, the minimization problem is solved by genetic algorithm (GA), and the constraints are handled by the GA itself. Here, real coded GA is implemented. Following Kalyanmoy[12], simulated binary crossover and parameter-based mutation operator is utilized; and the constraints are handled as follows: first all constraints are transformed to the form $g >= 0$ and normalized. The fitness function is defined as

$$F(\mathbf{x}) = \begin{cases} y(\mathbf{x}) & \text{if } \mathrm{g}_j(\mathbf{x}) \geq 0 \ \ \forall \mathrm{j}=1,2,...,\mathrm{m} \\ y_{\max} + \sum_{j=1}^{m} \langle g_j(\mathbf{x}) \rangle & \text{otherwise} \end{cases}, \tag{16}$$

where $m$ is the number of the constraints, and $\langle\ \rangle$ denotes the absolute value of the operand if the operand is negative, and returns a value zero otherwise. The parameter $y_{\max}$ is the objective function value of the worst feasible solution in the population.



Downloaded by TURKISH AEROSPACE INDUSTRIES (TAI) on May 2, 2023 | http://arc.aiaa.org | DOI: 10.2514/6.2012-967

Downloaded by TURKISH AEROSPACE INDUSTRIES (TAI) on May 2, 2023 | http://arc.aiaa.org | DOI: 10.2514/6.2012-967

### C. Framework of the Optimization System

In this research, a Kriging-based optimization system is developed. First, several initial sample points are generated in the design space using design of experiments (DoE). Here, we use the Latin hypercube sampling (LHS); then the samples are observed with parallel computing to save total clock time; after that, the Kriging models are constructed both for objective function and constraints (geometry constraints excluded), then the Kriging models are refined repetitively by infilling one or more new points obtained with GA under some specified infill criteria; this iteration terminates until some stop criteria meet, for instance, the function evaluation budgets or EI exceeds some specified value. The framework of the optimization is as follows:

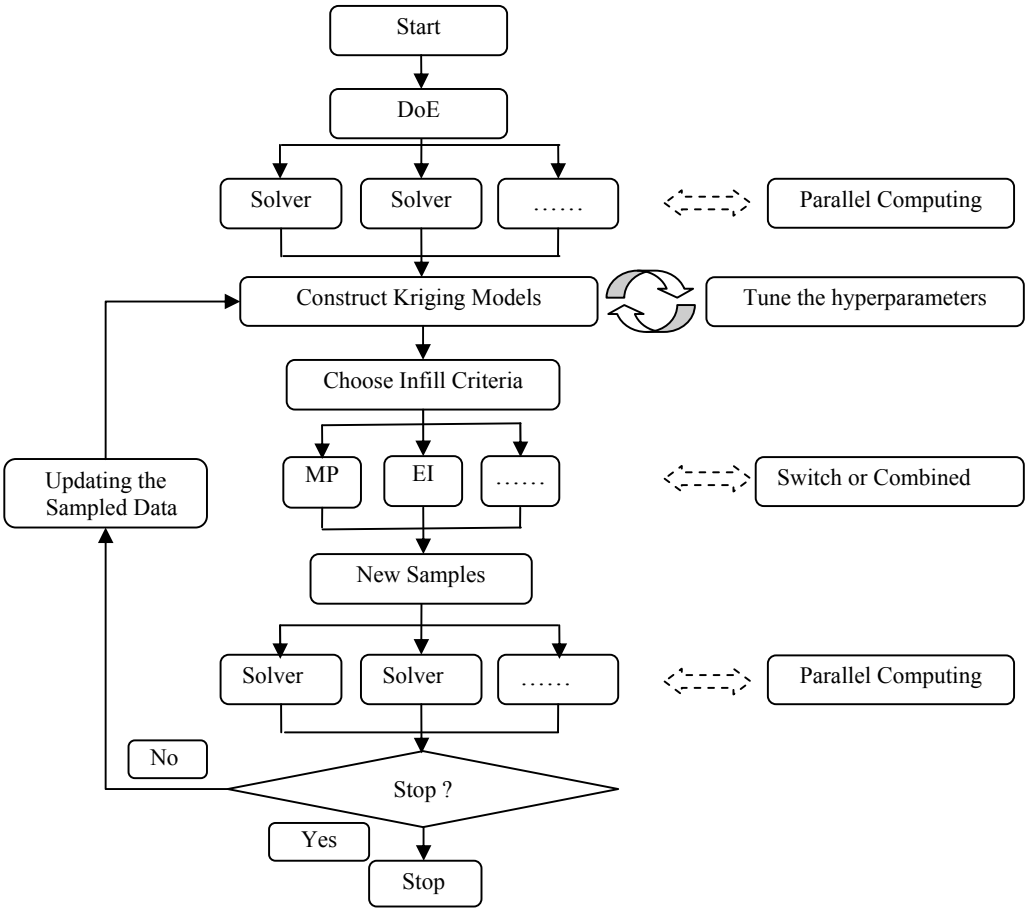


## IV. Numerical examples

### A. Globality Test of Kriging-Based Optimization

Is the Kriging with the expected improvement a global optimization method? Can it converge to the global optimum no matter how few initial sample points are given? Here we employ an analytical function to test its globality. Note that only the EI infill criterion is used.

The analytical function tested here is

$$f(x) = e^{-x} + \sin(x) + \cos(3x) + 0.2x + 1.0, \quad x \in [0.2, 6.0]. \tag{17}$$

Only two initial sample points $x_1 = 0.3, x_2 = 0.5$ are given. The process of the search is described in Fig.1. Note that the Kriging prediction, EI and root mean squared error (RMSE) are presented after every two cycles of modeling refinement. The function is extremely deceptive and the initial condition cannot be worse since the samples cannot be less and the location of the samples is as far as possible to the global optimum. In spite of this, the optimizer did

find the global optimum after 10 cycles of model refinements. This example further convinced us that combining with the EI infill criterion, the Kriging-based optimizer is a global optimizer.

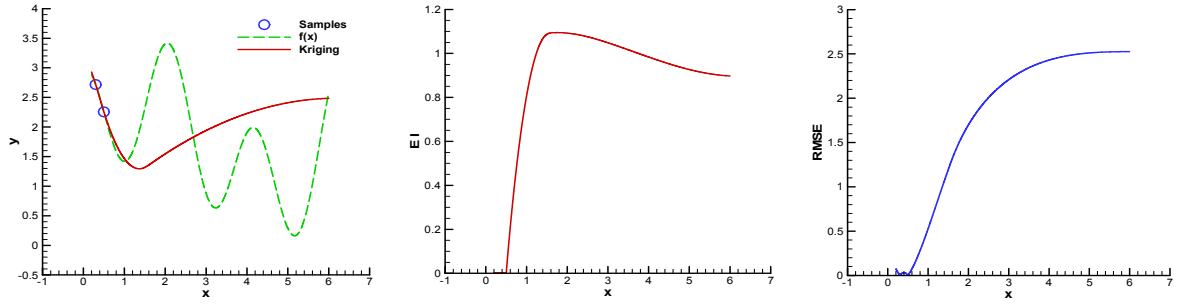


a) $n_s^{ini} = 2, n^{add} = 0$

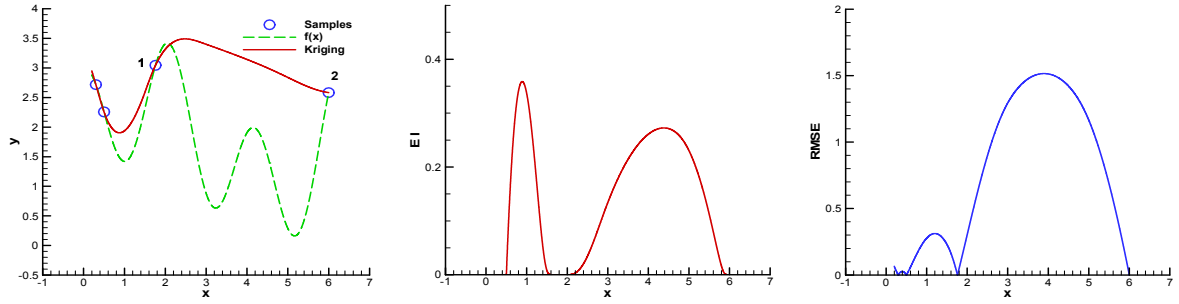


b) $n_s^{ini} = 2, n^{add} = 2$

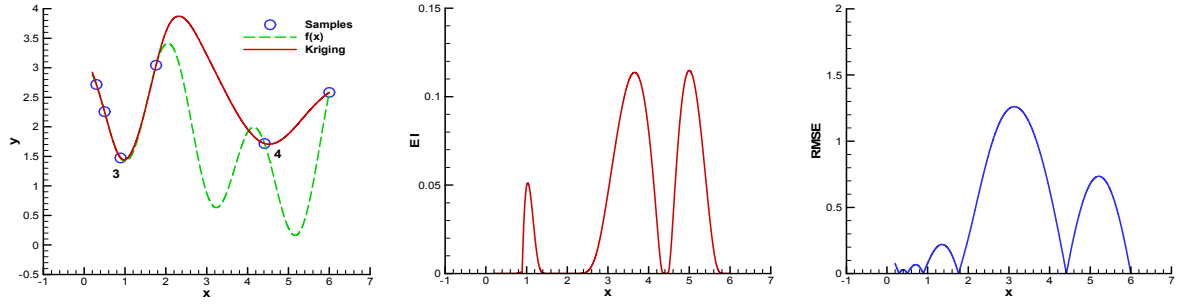


c) $n_s^{ini} = 2, n^{add} = 4$

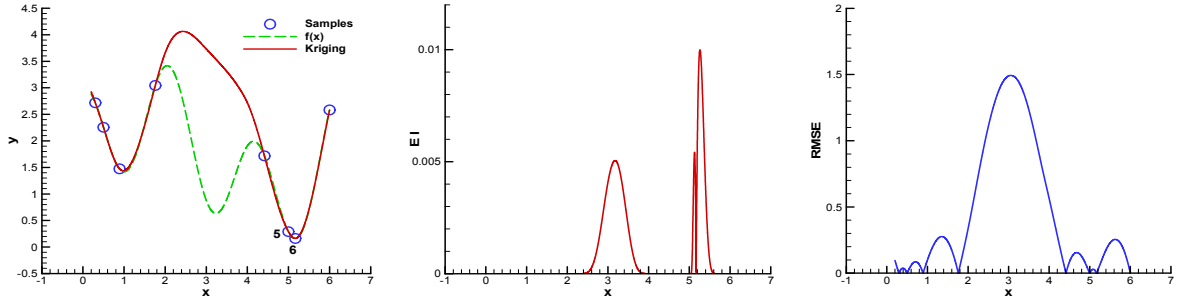


d) $n_s^{ini} = 2, n^{add} = 6$

Downloaded by TURKISH AEROSPACE INDUSTRIES (TAI) on May 2, 2023 | http://arc.aiaa.org | DOI: 10.2514/6.2012-967

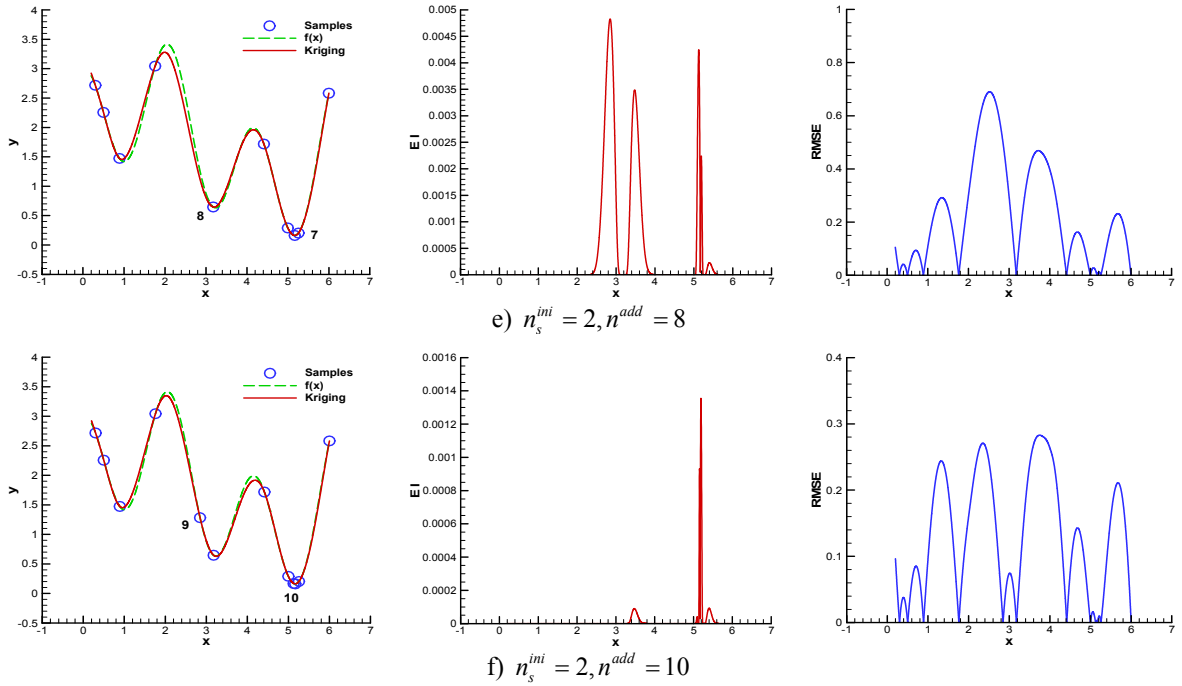


e) $n_s^{ini} = 2, n^{add} = 8$

f) $n_s^{ini} = 2, n^{add} = 10$

**Figure 1. The process of the search using Kriging-based optimizer**

## B. The Problem of the Size for Kriging-Based Optimization

It is well known that there exists a bottleneck of the surrogate-based optimization called "curse of dimensionality". For example, to build a reasonably accurate second-order polynomial response surface, the required number of sample points is proportional to $n_v^2$. However, there is no such limitation of the initial sample points for Kriging. The larger the number of design variables, the more sample points are needed. From our literature survey, few works can be found for this issue. In this paper, we are trying to give preliminary results of this problem.

This is easier said than done, since it is hard to decide when to stop the iteration, i.e. it is hard to find stopping criteria of the Kriging-based optimization for fair comparison. In this study, we used the "relative stopping criterion"[22]:

$$\max EI(\mathbf{x}) < \rho(f_{\max} - f_{\min}) \ , \tag{18}$$

where $f_{\max}, f_{\min}$ denote the maximum and minimum value of the objective function in the sampled data, respectively, and $\rho = 0.1\%$ is used here. The iteration stops until Eq. (18) is met for 3 times consecutively.

The Rosenbrock function[①] is used as the test function:

$$f(\mathbf{x}) = \sum_{k=1}^{n_v-1}\left[100\left(x_{k+1} - x_k^2\right)^2 + \left(x_k - 1\right)^2\right] \ , \ -5 \le x_k \le 10 \ , \ k = 1, 2, \cdots, n_v \ . \tag{19}$$

There are several local optima for this function, and the global optima is $\mathbf{x}^* = (1, \cdots, 1), f(\mathbf{x}^*) = 0$.

The optimizations are exercised for 2 to 40 dimensional problems. For each dimensionality, the optimization is repeated for 10 times and the averaged final number of sample points is utilized, with the initial number of sample points set to 2 and 5 times of the dimensionality respectively. The results are given in Fig. 2.

From Fig. 2 one can see that for both types of initial sampling, the required number of sample points (or function evaluation) increases nearly linearly as the number of dimensionality is increased. Note that when the number of dimensionality is larger than 10, the slope becomes smaller. However, this is still an open issue, and more study should be carried out in future.

[①] http://www-optima.amp.i.kyoto-u.ac.jp/member/student/hedar/Hedar_files/TestGO_files/Page2537.htm



Downloaded by TURKISH AEROSPACE INDUSTRIES (TAI) on May 2, 2023 | http://arc.aiaa.org | DOI: 10.2514/6.2012-967

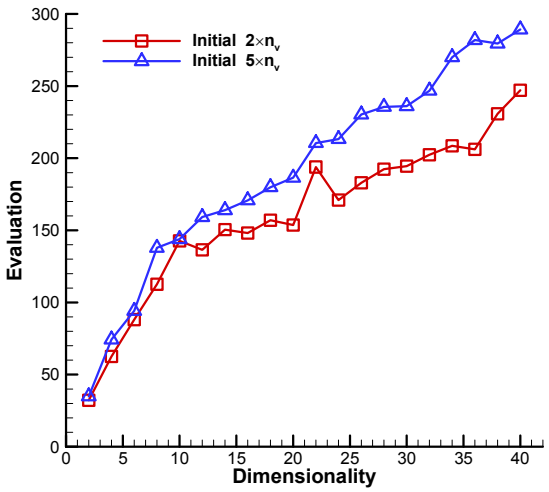


**Figure 2. Number of function evaluations needed for different number of design variables**

### C. Comparison of Kriging-Based and Response-Surface-Based Optimizers

The iterative response-surface-based optimizer is implemented to be compared with the Kriging-based optimizer. These two optimizers are compared for the drag minimization of an RAE2822 airfoil. The mathematical model is as following

$$\begin{aligned} Objective &: \text{Minimize} \quad c_d \\ s.t. &: (1)\ c_l \geq c_{l0} \\ &: (2)\ |c_m| \leq |c_{m0}| \\ &: (3)\ Thickness \geq Thickness_0 \end{aligned}, \tag{20}$$

where $Thickness_0$ denotes the maximum thickness of the baseline airfoil. 10 Hicks-Henne[21] shape functions are used to deform the airfoil, with 5 on the lower and upper surfaces, respectively; the amplitude of the functions are designated as design variables, hence, we have 10 design variables in total.

For the Kriging-based optimizer, 20 initial sample points are generated by LHS. EI as well as MP infill criteria are used simultaneously, thus two points are infilled to refine the surrogate models at each iteration.

For the RSM-based optimizer, we used the second-order polynomials to construct the response surfaces. There are $n = (n_v + 2)(n_v + 1)/2$ coefficients for $n_v$ variables. To obtain a reasonably accurate response surface, $1.5n$ sample points are needed for relatively small problems (5-10 variables) [10]. Hence, 99 initial sample points are generated by LHS in this example. Similar to the Kriging-based optimizer, once the response surface is constructed, the constrained optimization problem is solved using genetic algorithm. And the response surfaces are refined repetitively by infilling the newly sampled data. This iteration is terminated until the evaluation budget exceeds 15 times of the dimensionality.

Table 1 shows the optimization results of the two optimization methods. The two optimized and baseline airfoils and the corresponding pressure coefficient distributions are compared in Fig.3. Figure 4 shows the convergence history of the two optimizers. Obviously, the Kriging-based optimization method gives higher drag reduction percentage with much higher efficiency. This confirms the superiority of Kriging over the RSM, and demonstrates that the Kriging-based optimizer is more likely to find the global optimum.



Downloaded by TURKISH AEROSPACE INDUSTRIES (TAI) on May 2, 2023 | http://arc.aiaa.org | DOI: 10.2514/6.2012-967

**Table 1 Optimization results of the RAE2822 airfoil**

| | $c_d$ | $c_l$ | $\lvert c_m \rvert$ | *Thickness* | *Runs of flow solver* |
|---|---|---|---|---|---|
| Baseline | 100 | 100 | 100 | 100 | - |
| Kriging | 72.4 (-27.6%) | 100.6 (+0.6%) | 94.0 (-6.0%) | 100.0 (+0.0%) | 52 |
| RSM | 75.1 (-24.9%) | 101.9 (+1.9%) | 92.9 (-7.1%) | 100.0 (+0.0%) | 150 |

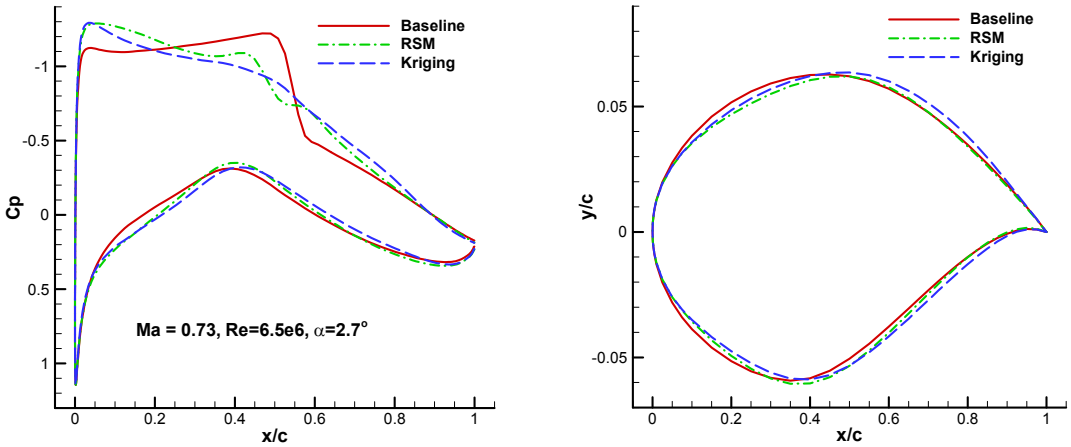


**Figure 3. Comparison of pressure coefficient distributions and geometries of the optimized and baseline airfoils.**

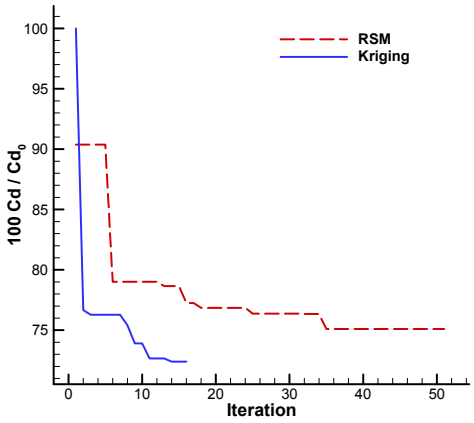


**Figure 4. Convergence history of the Kriging- and RSM-based optimizers**

### D. Kriging-Based Inverse Design of Transonic Airfoils

A Kriging-based single- and multi-point inverse design method is developed and investigated. Compared with the drag minimization of an airfoil based on Kriging models, the MP sampling refinement criterion is used instead of EI, since the inverse design is a local optimization problem. The objective function of the inverse design problem is:

$$J = \sum_{B_w} \left( C_p - C_{p0} \right)^2 , \tag{21}$$



Downloaded by TURKISH AEROSPACE INDUSTRIES (TAI) on May 2, 2023 | http://arc.aiaa.org | DOI: 10.2514/6.2012-967

where $C_p$ is the pressure coefficient of the current airfoil, and $C_{p0}$ is the pressure coefficient of the target airfoil; $B_w$ is the wall boundary.

For multi-point inverse design problems, the weighted-sum method is used:

$$J_{Total} = \sum_{i=1}^{N_m} \omega_i J_i \ , \tag{22}$$

where $N_m$ is the number of design points, $\omega_i$ is the corresponding weight.

Kulfan's CST[20] method is used to represent the airfoils instead of the Hicks-Henne bump functions. Unlike gradient-based inverse design methods, the design space should be designated instead of an initial airfoil. We first prescribe a "thick" shape and a "thin" shape, and then the two shapes are fitted by CST. We treat the CST parameters of the "thin" shape as the lower bound of the design variables, while the parameters of the "thick" shape as the upper bound. For real engineering problems, the geometry of the target airfoil is unknown, hence, one have to first prescribe the "thick" and "thin" shapes that covering the unknown target airfoil. As an example, the design space of the inverse designs in this paper is obtained by the 2 shapes shown in Fig. 5, and 19 design variables were used.

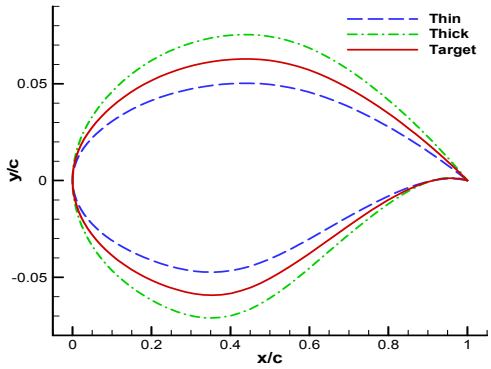


**Figure 5. The shapes to determine the design space**

1) Single Point Inverse Design

Our target is to obtain the REA2822 airfoil when given its pressure coefficient distribution on the airfoil boundary at the flow condition of $Ma = 0.73$, $\alpha$=2°, $\mathrm{Re} = 6.5 \times 10^6$ .

Figure 6 and 7 show the comparison of pressure coefficient distributions and geometries of the target airfoil and designed airfoil, respectively. We see that both the geometry of the designed airfoil and its pressure coefficient coincide well with the target airfoil's. Figure 8 shows the convergence history of the objective function, note that the square symbols ahead of the vertical line denote the initial sample points.

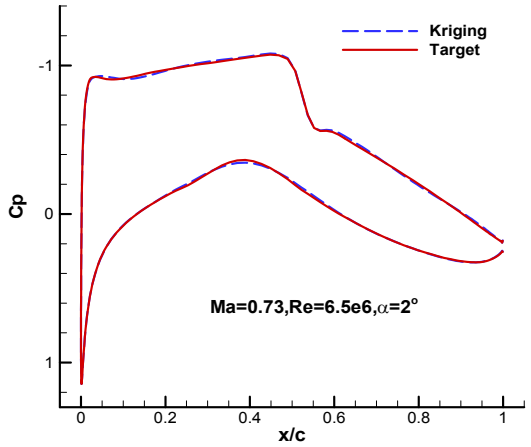


**Figure 6. Comparison of the pressure coefficient distributions**

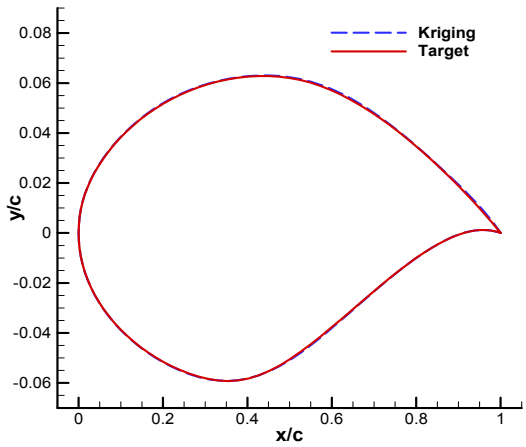


**Figure 7. Comparison of the geometries**



Downloaded by TURKISH AEROSPACE INDUSTRIES (TAI) on May 2, 2023 | http://arc.aiaa.org | DOI: 10.2514/6.2012-967

Downloaded by TURKISH AEROSPACE INDUSTRIES (TAI) on May 2, 2023 | http://arc.aiaa.org | DOI: 10.2514/6.2012-967

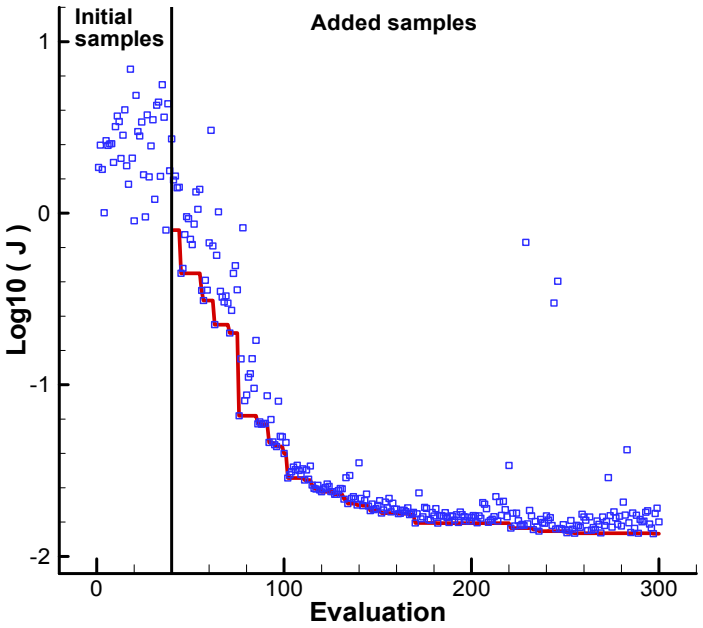


**Figure 8. Convergence history of the objective function for single point inverse design**

2) Two-Point Inverse Design

The pressure coefficient distributions on the boundary of the RAE2822 airfoil at the 2 flow conditions are given:

$$\begin{aligned} &\textit{design point 1}: \quad \text{Ma=0.73, Re=6.5e6, } \alpha=2.0^{o} \\ &\textit{design point 2}: \quad \text{Ma=0.70, Re=6.5e6, } \alpha=2.38^{o} \end{aligned} \quad . \tag{23}$$

In the equation (21), $\omega_1$ is set to 0.6, and $\omega_2$ 0.4 for this problem.

Figure 9 and 10 show the comparison of pressure coefficient distributions of designed airfoil and the target airfoil, and Fig. 11 shows the comparison of the geometries. It is showing that both the geometry of the designed airfoil and its pressure coefficients coincide well with the target airfoil's. Figure 12 shows the convergence history of the weighted-sum objective function and objective functions of the 2 design points.

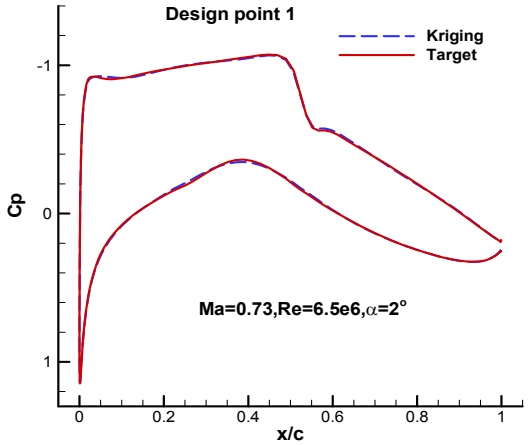


**Figure 9. Comparison of the pressure coefficient distributions at design point 1**

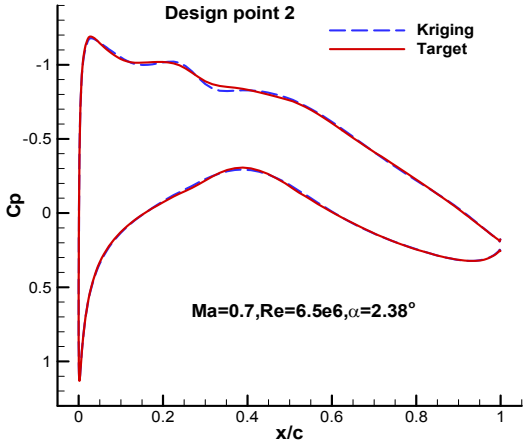


**Figure 10. Comparison of the pressure coefficient distributions at design point 2**

Downloaded by TURKISH AEROSPACE INDUSTRIES (TAI) on May 2, 2023 | http://arc.aiaa.org | DOI: 10.2514/6.2012-967

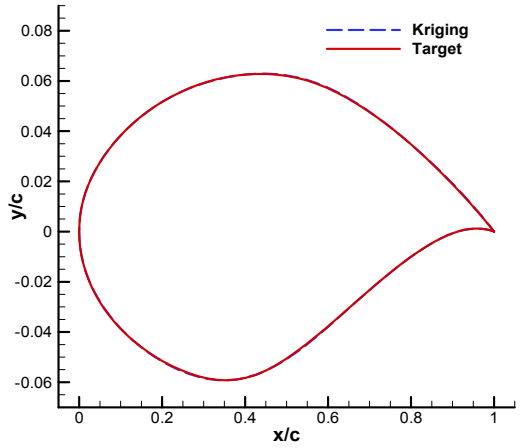


**Figure 11. Comparison of the shapes of the designed airfoil and target airfoil.**

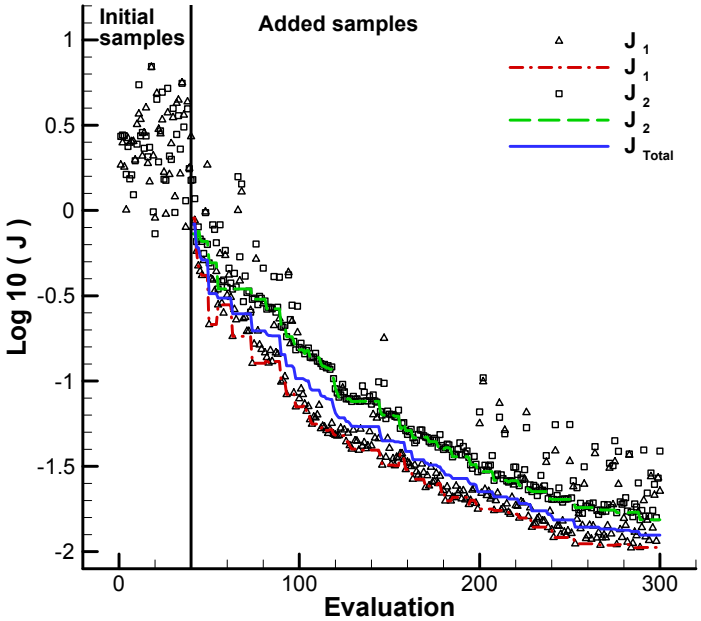


**Figure 12. Convergence history of the objective functions for two point inverse design**

## V. Conclusions

Several key issues for Kriging-based optimization are addressed in this study. Some preliminary conclusions can be drawn as follow:

1. A one-dimensional function is used to test the globality of the Kriging with EI optimization method, the result further convinced us that it does able to find the global optimum.
2. With the increase of the design variable, the number of sample points needed to sufficiently explore the design space grows rapidly, but the growing order is almost linear and is less than the polynomial response surface. However, this is only a preliminary research, and further research should be done.
3. The Kriging-based optimization method is compared with the RSM based optimization method in the transonic airfoil drag minimization problem; the former outperforms the latter both in efficiency and drag reduction per-

centage. This confirms the superiority of Kriging over the RSM, and demonstrates that the Kriging based optimizer is really efficient and is more likely to find the global optimum.

4. A Kriging-based inverse design method is presented and investigated in this paper, and applied in the transonic airfoil inverse design both for single and multi point. The result confirms the capability of the Kriging model in the inverse airfoil design, but further work should be done for the inverse design of an unknown airfoil.

Future study will focus on the further study on the globability of the Kriging-based optimization for aerodynamic design, how to break through the "curse of dimensionality", and the inverse design of unknown airfoils.

## Acknowledgments

This research was sponsored by the National Natural Science Foundation of China (NSFC) under grant No. 10902088 and the Aeronautical Science Foundation under grant No. 2011ZA53008.

Downloaded by TURKISH AEROSPACE INDUSTRIES (TAI) on May 2, 2023 | http://arc.aiaa.org | DOI: 10.2514/6.2012-967

## References

[1]Forrester, A. I. J. and Keane, A. J., "Recent Advances in Surrogate-based Optimization," *Progress in Aerospace Sciences*, Vol. 45, 2009.

[2]Goto, Y., Jeong, S., Obayashi, S., and Kohama, Y., "Design Space Exploration of Supersonic Formation Flying Focusing on Drag Minimization," *Journal of Aircraft*, Vol. 45, No. 2, March-April 2008.

[3]Takenaka, K., Hatanaka, K., Yamazaki, W., and Nakahashi, K., "Multidisciplinary Design Exploration for A Winglet," *Journal of Aircraft*, Vol. 45, No. 5, September-Octpber 2008.

[4]Kanazaki, M., Tanaka, K., Jeong, S.,and Yamamoto, K.," Multi-Objective Aerodynamic Exploration of Elements' Setting for High-Lift Airfoil Using Kriging Model" *Journal of Aircraft*, Vol. 44, No. 3, May-June 2007.

[5]Hoyle, N., Bressloff, N. W., and Keane, A. J., "Design Optimization of A Two-Dimensional Subsonic Engine Air Intake," *AIAA Journal*, Vol. 44, No. 11, November 2006.

[6]Song, W. and Keane, A. J., "Surrogate-Based Aerodynamic Shape Optimization of A Civil Aircraft Engine Nacelle," *AIAA Journal*, Vol. 45, No. 10, October 2007.

[7]Kanazaki, M., Imamura, T., Jeong, S., and Yamamoto, K., "High-Lift Wing Design in Consideration of Sweep Angle Effect Using Kriging Mode," AIAA paper 2008-175, 2008.

[8]Kumano, T., Jeong, S., Obayashi, S., Ito, Y., Hatanaka, K. and Morino, H., "Multidisciplinary Design Optimization of Wing Shape for A Small Jet Aircraft Using Kriging Model," AIAA 2006-932,2006.

[9]Paiva, R. M., Carvalho, A. R. D., Crawford, C., and Suleman, A., "A Comparison of Surrogate Models in the Framework of an MDO Tool for Wing Design," AIAA-2009-2203,2009.

[10]Koch, P. N., Simpson, T.W., Allen, J. K. and Mistree, F., "Statistical Approximations for Multidisciplinary Design Optimization: the Problem of Size," *Journal of Aircraft,* Vol. 36, No. 1, January-February 1999.

[11]Xiong, J. T., "Response Surface-Based Aerodynamic Optimization design," Master's Dissertation, School of Aeronautics, Northwestern Polytechnical University, Xi'an, China, 2005.

[12]Kalyanmoy, D., "An Efficient Constraint Handling Method for Genetic Algorithms," *Computer Methods in Applied Mechanics and Engineering,* Vol. 186, 2000, pp.311-338.

[13]Jones, D. R., Schonlau, M., and Welch, W. J., "Efficient Global Optimization of Expensive Black-Box Functions," *Journal of Global Optimization,*volume.13, pp.455-492,1998.

[14]Song, W. P., Xu, R. F., Han Z. H., "Study On The Improved Kriging-Based Optimization Design Method," *27TH International Congress of The Aeronautical Science,* 2010.

[15]Simpson, T. W., Mauery, T. M., Korte, J. J., and Mistree, F., "Comparison of Response Surface and Kriging Models for Multidisciplinary Design Optimization," AIAA-98-4755,1998.

[16]Peter, J., Marcelet, M., Burguburu, S., Pediroda, V., "Comparison of Surrogate Models for the Actual Global Optimization of a 2D Turbomachinery Flow," *Proceedings of the 7th WSEAS International Conference on Simulation ,Modeling and Optimization,* Beijing, 2007, pp.46-51.

[17]Krige, D. G., "A Statistical Approach to Some Basic Mine Valuations Problems on the Witwatersrand," *Journal of the Chemical, Metallurgical and Mining Engineering Society of South Africa*, Vol. 52, No. 6, 1951, pp. 119-139.

[18]Matheron, G. M., "Principles of geostatistics," *Economic Geology*, Vol. 58, No. 8, 1963, pp. 1246-1266.

[19]Sacks, J., Welch, W. J., Mitchell, T. J., and Wynn, H. P., "Design and Analysis of Computer Experiments," *Statistical Science,* Vol. 4,1989, pp. 409-423.

[20]Kulfan, B. M., "Universal Parametric Geometry Representation Method," *Journal of Aircraft,* Vol. 45, No. 1 January-February 2008.

[21]Hicks, R. M., and Henne, P., "Wing Design by Numerical Optimization," *Journal of Aircraft*, Vol. 15, No. 7, 1978, pp. 407–412.

[22]Huang, D., Allen, T. T., Notz, W. I., and Miller, R. A., "Sequential Kriging Optimization Using Multiple-Fidelity Evaluations," *Structural and Multidisciplinary Optimization*, Vol. 32, pp. 369-382, 2006.